Optimization of Support Vector Machines Performance using OCT Images

R Loganathan, and S Latha*

Abstract—**Age-related macular degeneration (AMD) primarily affects individuals aged 50 and above. Analyzing optical coherence tomography (OCT) images for the presence of drusen is essential to diagnosing AMD. OCT produces accurate cross-sectional images that may identify retinal thinning and accumulation of fluid. Feature learning techniques, such as the Gray Level Co-occurrence Matrix (GLCM), Neighborhood Gray-Tone Difference Matrix (NGTDM), First Order Statistics, and Gray Level Run Length Matrix (GLRLM), enhance OCT image analysis by extracting texture features. The application of machine learning methodologies, including support vector machines (SVM), facilitates the automated evaluation and classification of AMD according to predetermined criteria. Integrating advanced processing technologies with OCT imaging for AMD diagnosis could potentially lead to improved patient outcomes and the preservation of visual acuity among the older adult population. In the study, linear SVM achieved perfect accuracy (1.0) with scaling and regularization. RBF SVM performed well, scoring 0.981, excelling with non-linear data. Polynomial SVM matched this score but was sensitive to cross-validation. Sigmoid SVM had the lowest performance, scoring 0.7736 when unscaled and 0.981 when regularized, indicating poor adaptability without preprocessing.**

Index Terms— **AMD, drusen, OCT image, texture analysis, SVM, accuracy, f1score**

I. Introduction

AGE-related macular degeneration (AMD) causes progressive blurred vision for various people, primarily impacting individuals aged 50 years and older. AMD affects over 200 million people globally and will reach 300 million by 2040. Older people are disproportionately affected by this condition [1]. Drusen, yellowish deposits beneath the retina, are key indicators of AMD. A non-invasive diagnostic method is optical coherence tomography, which can reveal issues such as fluid buildup, retinal thinning, and drusen formation within the retinal layers [2]. OCT plays a crucial role in AMD diagnosis and monitoring by providing detailed retinal images [3]. Ophthalmologists may now more easily diagnose retinal diseases due to automated retinal image processing in biomedical applications. Traditional therapies like pupil dilation are no longer necessary because of this elimination [4]. An important defining feature of AMD is the vascular destruction that occurs in the retina. The ageing process causes this condition, which results in the deterioration of the small veins, supplying the retina with oxygen and nutrients [5].

A broad spectrum of disorders and conditions has the potential to impact the eyes, leading to vision impairment or a substantial deterioration in visual acuity. There are several common visual illnesses and abnormalities, including cataracts, diabetic retinopathy, glaucoma, hypertensive retinopathy, myopia, and age-related macular degeneration [6]. Identification and diagnosis promptly are essential for effective treatment and vision preservation. An ideal solution to this issue would be a model that integrates deep learning (DL) and machine learning (ML) to differentiate between healthy eyes and those who are infected [7].

The creation of an approachable educational platform on eye disorders is essential, as various people suffer from degenerative diseases that cause blindness for which there is no treatment. Grouping multi-label OCT images helps diagnose eye diseases, but getting true OCT data, particularly for uncommon conditions, is difficult. The accuracy of the infected detection model is reduced by data scarcity and visual noise.

Recent advances in machine learning have dramatically improved OCT images for eye disease diagnosis. Voter classifiers like XGBoost, Support Vector Machines, Gradient Boosting, and Decision Trees, along with Random Forests, have proven effective in accurately identifying different retinal disorders in images. SVM, which utilizes multiple kernel functions such as linear, polynomial, and radial basis functions (RBF), helps diagnose AMD by distinguishing between healthy and infected AMD OCT images. Feature extraction methods like the Gray Level Co-occurrence Matrix (GLCM), Gray Level Run Length Matrix (GLRLM), Neighborhood Gray Tone Difference Matrix (NGTDM), and First Order Statistics are applied to an OCT image dataset and then combined to form a new dataset. Sigmoid, linear, Radial Basis Function (RBF), and polynomial SVM kernel functions are tested for multi-label OCT image classification to diagnose AMD. A lack of adequate and reliable OCT data for rare retinal illnesses makes accurate disease identification difficult. Comparison of SVM confusion matrices, accuracy, precision, and f1 score helps find the best AMD classifier. This study correlates four SVM kernels (linear, RBF, polynomial, and sigmoid) under identical conditions and investigates the combined effects of scaling, regularization, and cross-validation. It determines SVM performance accurately, quantifies the influence of preprocessing techniques, and provides practical advice for optimizing model performance.

Manuscript Received August 10, 2024; revised September 23, 2024.

R Loganathan is a PhD student of Department of Electronics and Communication Engineering, College of Engineering and Technology, SRM Institute of Science and Technology, Kattankulathur Campus, Chengalpattu 603203, Tamil Nadu, India. (e-mail: lr1054@srmist.edu.in)

S Latha* is an Associate Professor of the Department of Electronics and Communication Engineering, College of Engineering and Technology, SRM Institute of Science and Technology, Kattankulathur Campus, Chengalpattu 603203, Tamil Nadu, India. (Corresponding author to provide e-mail: lathas3@srmist.edu.in)

II. Related Works

Recent research has examined the possibility of predicting AMD using OCT images. Machine learning is being studied for several medical conditions, including AMD. Researchers used these algorithms to diagnose and predict various medical problems. Machine learning techniques are implemented using SVM, KNN, Random Forest, Logistic Regression, and Decision Tree algorithms [8].

Researchers survey AMD by utilizing a variety of datasets, which include OCT scans, fundus images, and hospital data. OCT image databases provide innovative methods for identifying and investigating this potentially blinding issue. Recently developed machine learning and deep learning in OCT image processing for retinal diagnostics are promising.

Harshini et al. demonstrated a voting classifier [9] with 98.79% accuracy. Shamsan et al. achieved 99.23% AUC utilizing hybrid techniques [10], and Esraa Hassan et al. used CNNs and modified ResNet models and Random Forest classifiers [11] to classify general OCT images with 99.2% accuracy. Amin Alqudah presented 98.7% accurate hybrid AI systems using machine learning and CNNs [12]. Xing Wei et al. accurately segmented retinal cysts 96.8% for therapeutic planning [13]. Venkatesan Rajinikanth et al. improved imaging for age-related macular degeneration categorization, attaining 93.67% accuracy [14]. Geetha Pavani classified neovascularization with 93.4% accuracy using extreme learning machine (ELM) classifiers [15]. Abdulrahman et al. employed Genetic Programming to select the Gabor filter, LBP, GLCM, histogram, and SURF for feature extraction, achieving 90.95% accuracy in detecting retinal abnormalities with SVM, outperforming traditional methods [16]. Venkatraman et al. utilized preprocessing and histogram of oriented gradients (HOG) feature extraction to classify OCT images based on fluid patterns, achieving 89.29% accuracy with KNN classification [17].

III. Methodology

A. Optimization Methods for Classification Leveraging Machine Learning

Classification, in particular, supervised learning, is highly suitable for the machine learning challenge of differentiating between typical OCT images and those exhibiting AMD. OCT scans assist in the diagnosis of AMD and other retinal disorders by offering detailed cross-sectional images of the retina. The objective is to ascertain whether the OCT images depict age-related macular degeneration signaling retinal structures or those that are normal. The input (OCT images) and output (diagnosis of normal or AMD) are explicitly specified under the principles of supervised learning [18]. Fig. 1 illustrates the process for classifying optical coherence tomography (OCT) images using SVM algorithms.

After importing the data and extracting the features, the model is constructed for AMD/normal categorization. To enhance the differentiation between age-related macular degeneration (AMD) and typical macular degeneration (OCT) in images, the model will undergo modifications, considering the nuances of medical image processing. At that point, the model would be more capable of differentiating between the two cases. These changes would not emphasize the features of OCT images or the clinical indications associated with AMD.

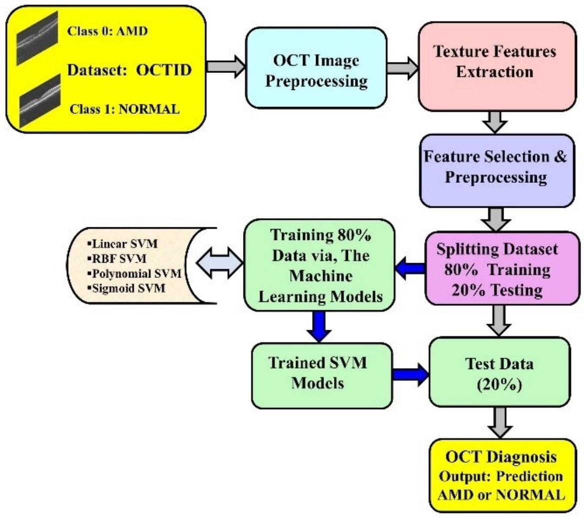

Fig. 1. OCT image classification model.

B. Support Vector Machine

SVM is used widely in data mining, machine learning, neural networks, and pattern recognition. SVM algorithms are used to represent the problem of defining two classes in feature space: normal and AMD, as shown in Fig. 2.

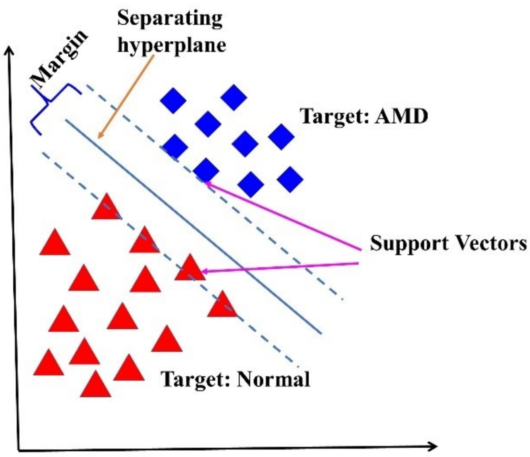

Fig. 2. SVM-based linear data classification

Support Vector Machines (SVM) employs the Maximum Margin Hyperplane (MMH) to partition the two data elements through the creation of numerous hyperplanes. Identifying the hyperplane with the greatest distance between data points and correctly categorizing them is realistic. Fig. 2 shows positive and negative hyperplanes, with the first type supporting positive data points and the latter supporting negative ones. When these hyperplanes are positioned optimally, the distance between them may be maximized. SVM solves regression and data classification optimization challenges. Hyperplane identifies and divides the data into positive and negative points and classifies them accordingly. The hyperplane that is illustrated herein symbolizes the anticipated decision boundary for the linear support vector machine.

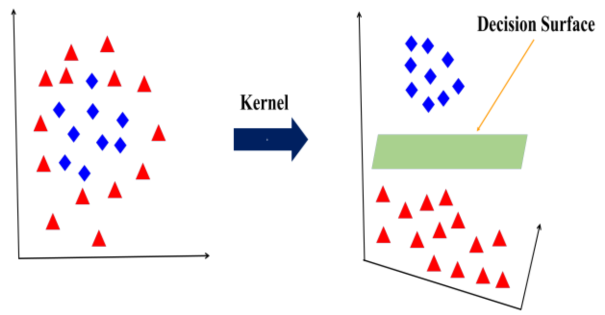

Fig. 3. SVM-based nonlinear data classification

Kernels translate nonlinear data into higher dimensions for SVM classification, as seen in Fig. 3. Several classes for the kernel function can be used for classification. Choosing the right kernel function is very important for correctly grouping data points. Applying the kernel function raises one class of data to a higher dimension, enabling decision surfaces to categorize data points. The significance of choosing the right kernel function for maximizing SVM classification performance is emphasized by this technique.

The primary principle is to create nonlinear separators. Classification using linear decision surfaces requires data transformation into a higher dimensional space. As shown in Fig. 3, a reformulation problem implicitly maps the data to this space. The method improves SVM's discriminative features by handling complicated data distributions more successfully.

The process of transforming data into a higher dimensional feature space, represented as F(x1, x2), is facilitated by the kernel function. Data points (x1, x2) can be separated linearly by this method. Thus, linear and nonlinear classifications may be performed using SVMs. To perform nonlinear classification, the kernel function projects dataset points into a higher dimensional feature space. Additionally, kernel functions are required to meet the stipulation delineated in Mercer's theorem [19].

Kernels are used in SVM for decision making the most common are linear, polynomial, RBF, and sigmoid, and they all have their unique uses in classification problems. Frequently employed kernel functions consist of:

Linear kernel: $$F(x_1, x_2) = (x_1 \cdot x_2) \tag{1}$$

Polynomial kernel: $$F(x_1, x_2) = (x_1^T \cdot x_2 \ + C)^d \tag{2}$$

RBF kernel: $$F(x_1, x_2) = e^{\frac{-\|x_1 - x_2\|^2}{2\sigma^2}} \tag{3}$$

Sigmoid kernel: $$F(x_1, x_2) = \tanh(\alpha x_1^T \cdot x_2 + \mathrm{C}) \tag{4}$$

The simplest kernel function is linear, which takes the inputs (x1 · x2) and uses an optional constant c to determine the linear kernel's inner product. Noise or inadequate feature representation causes nonlinear separability. Data is mapped into a separate space. The Polynomial kernel, utilizing mathematical function (2) instead of (x1 · x2), C balances training data fit and margin size. Large C has low training error but overfit, whereas small C has high error but underfit. The polynomial's degree d controls the model level of complexity. Higher degrees of d may provide more complicated overfitting models, whereas lower degrees may produce simpler underfitting models. Gaussian kernel, or Radial basis function (RBF) kernel, is equation (3), in this case, σ controls the spread of the kernel. The sigmoid kernel is given by equation (4), where α scales input data and C regulates the mapping threshold.

C. Dataset Acquisition

Open Access OCT Image Database (OCTID) is used for the study [20]. In the spectrum domain, the small database has about 250 volumetric OCT images. The two different groups, normal and age-related macular degeneration (AMD), are carefully segregated for analytical reasons. There are two categories: 21.07% AMD and 78.93% Normal. 206 out of 261 instances in OCTID belong to the Normal group, while 55 belong to the AMD category as shown below in Fig. 4.

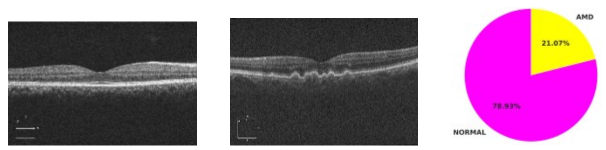

(a) Normal (b) Dry AMD (c) % for 2 classes

Fig. 4. OCTID in a row for (a) normal, (b) drusen or dry AMD, and (c) % for 2 classes.

Data Preprocessing

The proposed method retrieves OCT images from a database, selecting and saving them in .jpeg format during processing. Grayscale OCT images encode reflectance data, with each pixel's intensity and luminosity represented by a single value. These images distinguish luminance levels through encoded bytes or words assigned to each pixel. The OCT image dataset has 261 images from 2 classes. The dataset image is scaled to 100x100 for each image.

Feature Extraction

In medical image analysis research, Optical Coherence Tomography (OCT) image extraction of specific features is essential. The system computes several aspects, including texturing qualities and fundamental statistical values, by using certain algorithms. In particular, the Neighborhood Gray Tone Difference Matrix (NGTDM), the Gray Level Run Length Matrix (GLRLM), the Gray Level Co-occurrence Matrix (GLCM), and the first-order statistics are illustrative of these features. Both classes possess a combined total of 33 features shown in Table I. The next step is to carefully examine the OCT images in the assigned files, extracting and classifying the relevant characteristics for the study.

Feature Selection

SelectKBest method utilizing ANOVA F values via f_classif ranks features by target prediction significance. A data frame orders feature by importance for machine learning improvements. The analysis of prediction models is significantly enhanced using this method. OCT retinal images were separated using the train test split algorithm into 20% testing and 80% training across two categories. After processing the training data, an SVM classifier classified images as AMD or Normal. Training and evaluating the dataset for image classification was made simpler using this method.

D. Evaluation Metrics

Accuracy: Measures the classifier's ability to accurately predict classifying AMD and Normal instances with OCT images to establish the accurate prediction ratio of the dataset sample size.

Recall: Represents the proportion of positive predictions (e.g., AMD cases) that are correctly identified as positive, crucial for accurate diagnosis in medical imaging, particularly for detecting AMD in OCT images.

Precision: Reflects the proportion of true positive and true negative cases (both Normal and AMD) correctly classified as positive, providing insight into the classifier's performance on accurately identifying positive cases.

F1-Score: Evaluates the classifier's effectiveness in categorizing normal and AMD cases in OCT images by computing accuracy and recall as a harmonic mean.

TABLE I
DESCRIPTION OF THE OCTID FOR 33 FEATURES

Description	Features	Dataset Summary
FOS	1. Mean Intensity, 2. Standard Deviation 3. Median, 4. Mean Absolute Deviation 5. Relative Mean Absolute Deviation 6. Root Mean Square, 7. Variance 8. Minimum, 9. Maximum, 10. Skewness 11. Kurtosis, 12. Entropy, 13. Interquartile Range	No. of Features: 13 No. of Instances: 261 No. of Classes: 2 Missing Values: No missing values Feature Type: Numeric
GLCM	1. Contrast, 2. Dissimilarity, 3. Homogeneity 4. Energy, 5. Correlation 6. Angular Second Moment 7. Texture Entropy, 8. Maximum Probability	No. of Features: 8 No. of Instances: 261 No. of Classes: 2 Missing Values: No missing values Feature Type: Numeric
GLRLM	1. Short Run Emphasis, 2. Long Run Emphasis 3. Gray Level Non-Uniformity 4. Run Length Non-Uniformity, 5. Run Percentage 6. Low Gray Level Run Emphasis 7. High Gray Level Run Emphasis	No. of Features: 7 No. of Instances: 261 No. of Classes: 2 Missing Values: No missing values Feature Type: Numeric
NGTDM	1. Coarseness, 2. Contrast 3. Busyness, 4. Complexity 5. Strength	No. of Features: 5 No. of Instances: 261 No. of Classes: 2 Missing Values: No missing values Feature Type: Numeric

E. Experimental Setup

Four Support Vector Machine (SVM) models were tested under different preprocessing and validation conditions. The models comprised sigmoid, polynomial, linear, and RBF SVMs. Raw data (without preprocessing or validation), scaled data, scaled and regularized data, and CV scaled and regularized data were the four experimental scenarios. Each model was evaluated using training accuracy, testing accuracy, best score, F1 score, accuracy, recall, and ROC AUC. Data scaling normalizes feature values, whereas regularization prevents overfitting. In cross-validation, the dataset was folded five times. The model was trained on four folds and verified on five. It was averaged over all five folds. The studies employed Python, Scikit-learn for machine learning, Pandas for data processing, Matplotlib, and Seaborn for visualization [21]. This setup enabled SVM model comparisons and revealed how preprocessing and validation affect model performance.

IV. Results and Discussion

AUC, Precision, Sensitivity, Accuracy, and the Confusion Matrix were used to compare how well the models did on OCT images as part of the study. The True Positives, Negatives, and False groups in the Confusion Matrix showed the link between the expected and true classes. The best OCT image-based AMD detection method was found in this work, revealing novel machine-learning applications in OCT.

Table II compares the performance of support vector machines (SVMs) with and without scaling and cross-validation. Linear SVM achieves optimal test accuracy and metrics. The RBF SVM model has high accuracy but low specificity. Although the sigmoid SVM has lower accuracy due to large misclassification rates and poor specificity, the polynomial SVM demonstrates excellent performance.

Regularization and scaling are compared with SVM performance in Table III. Linear SVM is 100% accurate when the best value is set to 1.0. The RBF and polynomial SVMs show excellent test accuracy with C = 10, gamma = 0.1, and (C = 0.1, degree = 2), respectively. Additionally, sigmoid SVM performs exceptionally well when C = 100 and gamma = auto. This analysis evaluates SVM models with various kernels and hyperparameters. It includes heatmaps showing accuracy for RBF kernels across C and gamma and for polynomial kernels across C, gamma, and degree. The optimal parameters and performance metrics are reported. Fig. 5 shows accuracy across different SVM kernels: (a) linear SVM with C; (b) RBF SVM with C and gamma; (c) polynomial SVM with C, gamma, and degree; (d) sigmoid SVM with C.

TABLE II
COMPARISON OF SVM MODEL PERFORMANCE WITHOUT CROSS-VALIDATION: SCALED

Model	Linear / Nonlinear	Train Accuracy	Test Accuracy	Sensitivity / TPR	Specificity / TNR	Misclassify rate	FPR / Fall-Out	FNR/ Miss Rate
Linear SVM (LSVM)	Linear	0.9760	1.0000	1.0000	1.0000	0.0000	0.0000	0.0000
RBF SVM (RSVM)	Nonlinear	0.9760	0.9623	0.9756	0.9167	0.0377	0.0833	0.0244
Polynomial SVM (PSVM)	Nonlinear	0.9904	0.9811	0.9756	1.0000	0.0189	0.0000	0.0244
Sigmoid SVM (SSVM)	Nonlinear	0.7933	0.7736	1.0000	0.0000	0.2264	1.0000	0.0000

TABLE III
COMPARISON OF SVM MODEL PERFORMANCE WITHOUT CROSS-VALIDATION: SCALED & REGULARIZATION

Model	Linear / Nonlinear	Best Parameters	Train Accuracy	Test Accuracy	Sensitivity / TPR	Specificity / TNR	Misclassify rate	FPR / Fall-Out	FNR/ Miss Rate
Linear SVM	Linear	C: 1.0	0.9760	1.0000	1.0000	1.0000	0.0000	0.0000	0.0000
RBF SVM	Nonlinear	C: 100, Gamma:0.1	0.9760	0.9811	1.0000	0.9167	0.0189	0.0833	0.0000
Polynomial SVM	Nonlinear	C: 0.1, Degree: 2	0.9760	0.9811	1.0000	0.9167	0.0189	0.0833	0.0000
Sigmoid SVM	Nonlinear	C: 100, Gamma: auto	0.9760	1.0000	1.0000	1.0000	0.0000	0.0000	0.0000

TABLE IV
COMPARISON OF SVM MODEL PERFORMANCE WITH CROSS-VALIDATION: SCALED & REGULARIZATION

Model	Linear / Nonlinear	Best Parameters	Best Score	Train Accuracy	Test Accuracy	Sensitivity / TPR	Specificity / TNR	Misclassify rate	FPR / Fall-Out	FNR/ Miss Rate
Linear SVM	Linear	C: 100	0.976	0.9904	1	1.0000	1.0000	0.0000	0.0000	0.0000
RBF SVM	Nonlinear	C: 1000, Gamma: 0.01	0.9806	0.9904	0.9811	0.9756	1.0000	0.0189	0.0000	0.0244
Polynomial SVM	Nonlinear	C: 0.1, Degree: 5	0.976	0.976	0.9434	0.9512	0.9167	0.0566	0.0833	0.0488
Sigmoid SVM	Nonlinear	C: 10, Gamma: 'auto'	0.9758	0.976	0.9811	1.0000	0.9167	0.0189	0.0833	0.0000

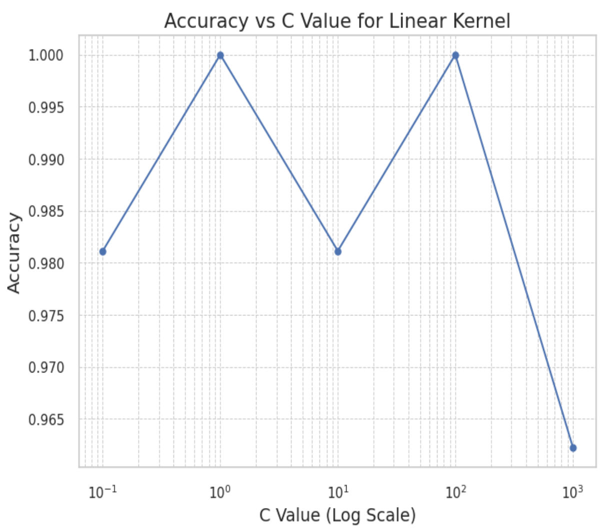

(a) Accuracy vs C value for linear SVM

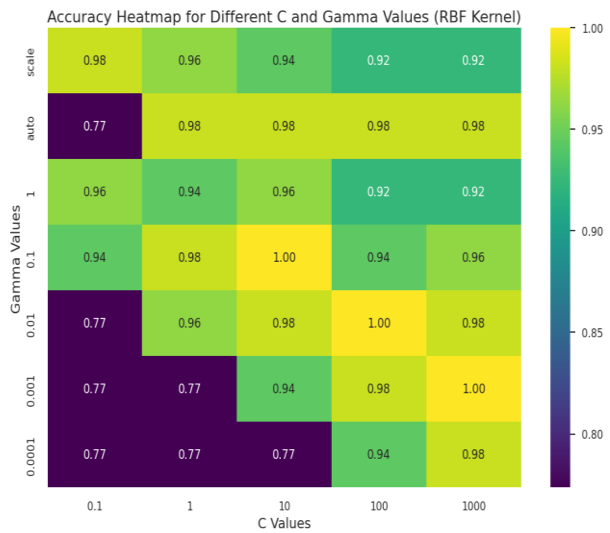

(b) Accuracy vs C value vs gamma value for RBF SVM

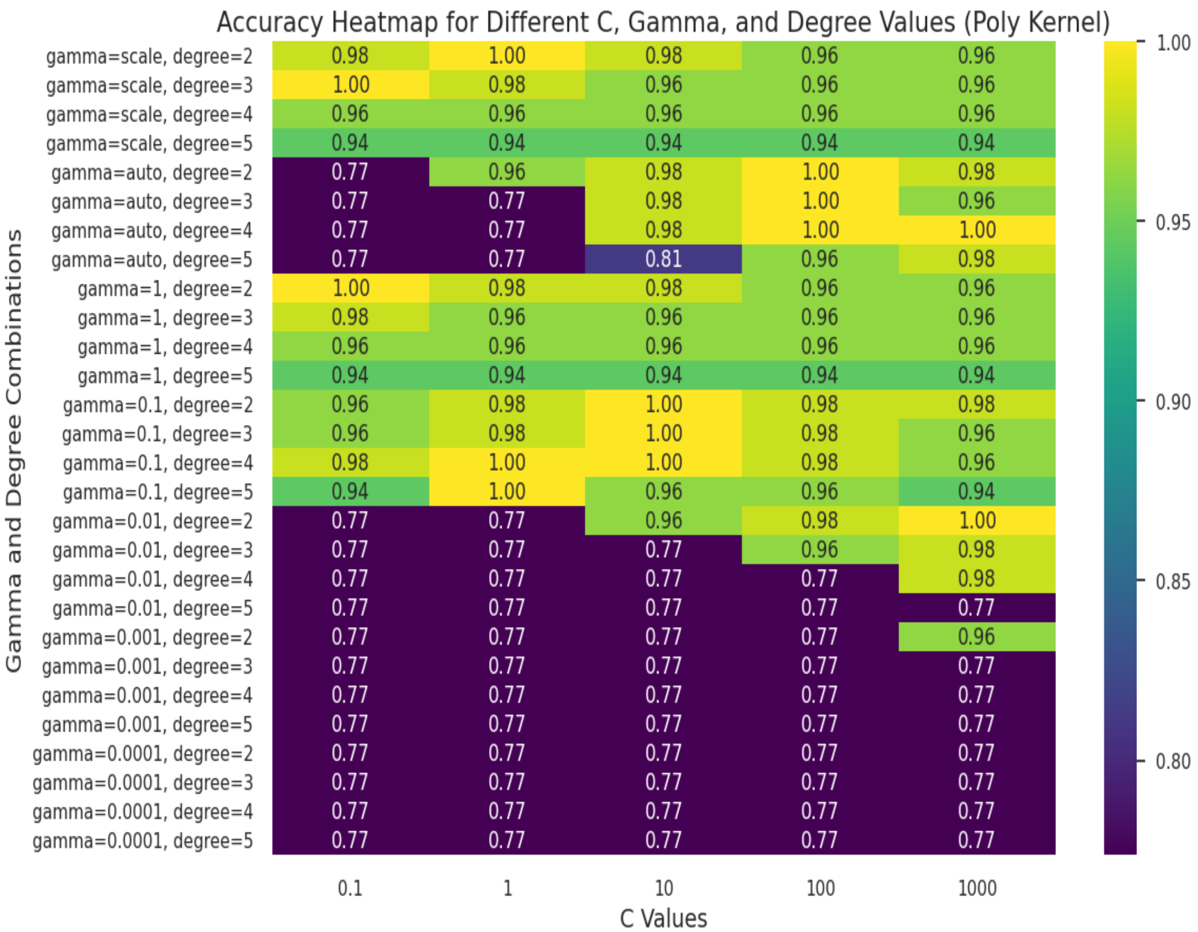

(c) Accuracy for polynomial SVM: C, gamma, and degree Values

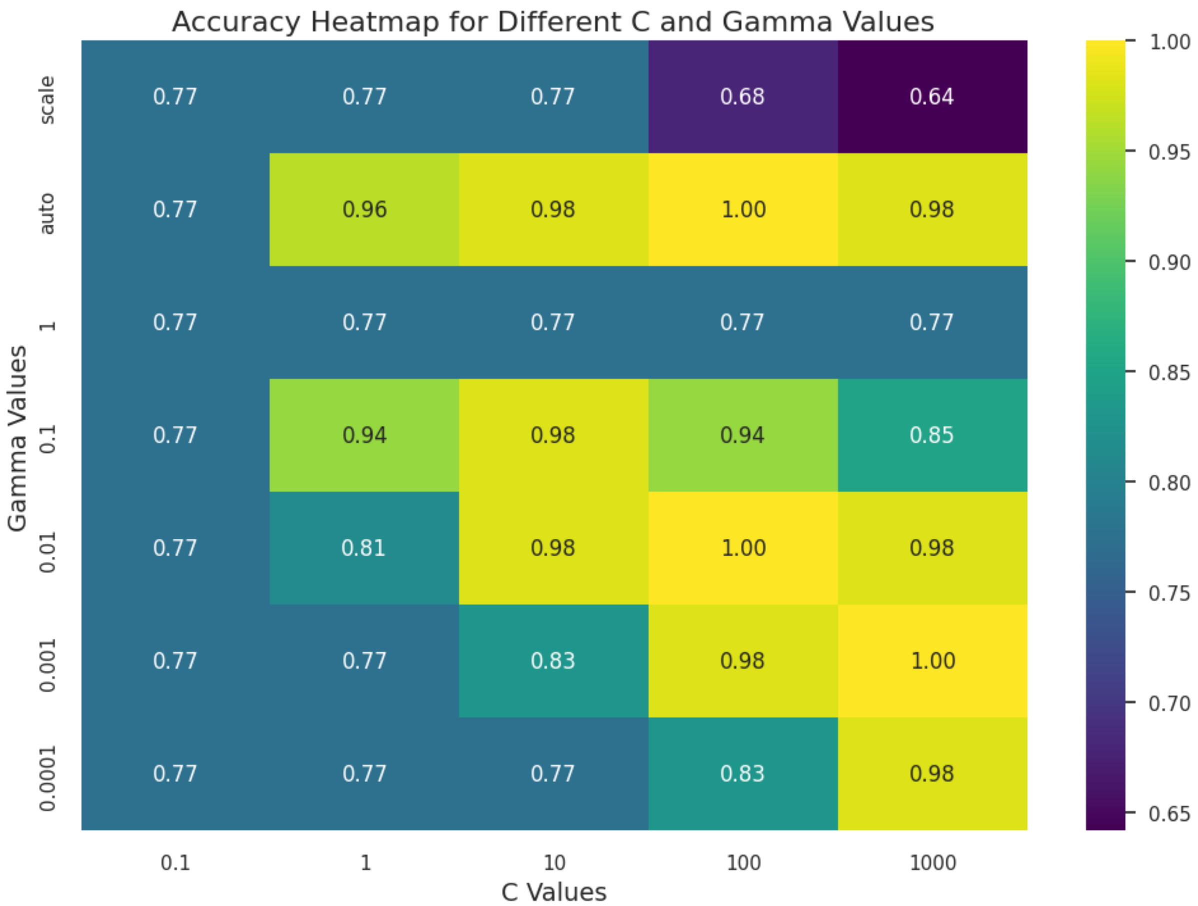

(d) Accuracy vs C value for sigmoid SVM

Fig. 5. Accuracy heatmap for various SVM kernels across hyperparameter values

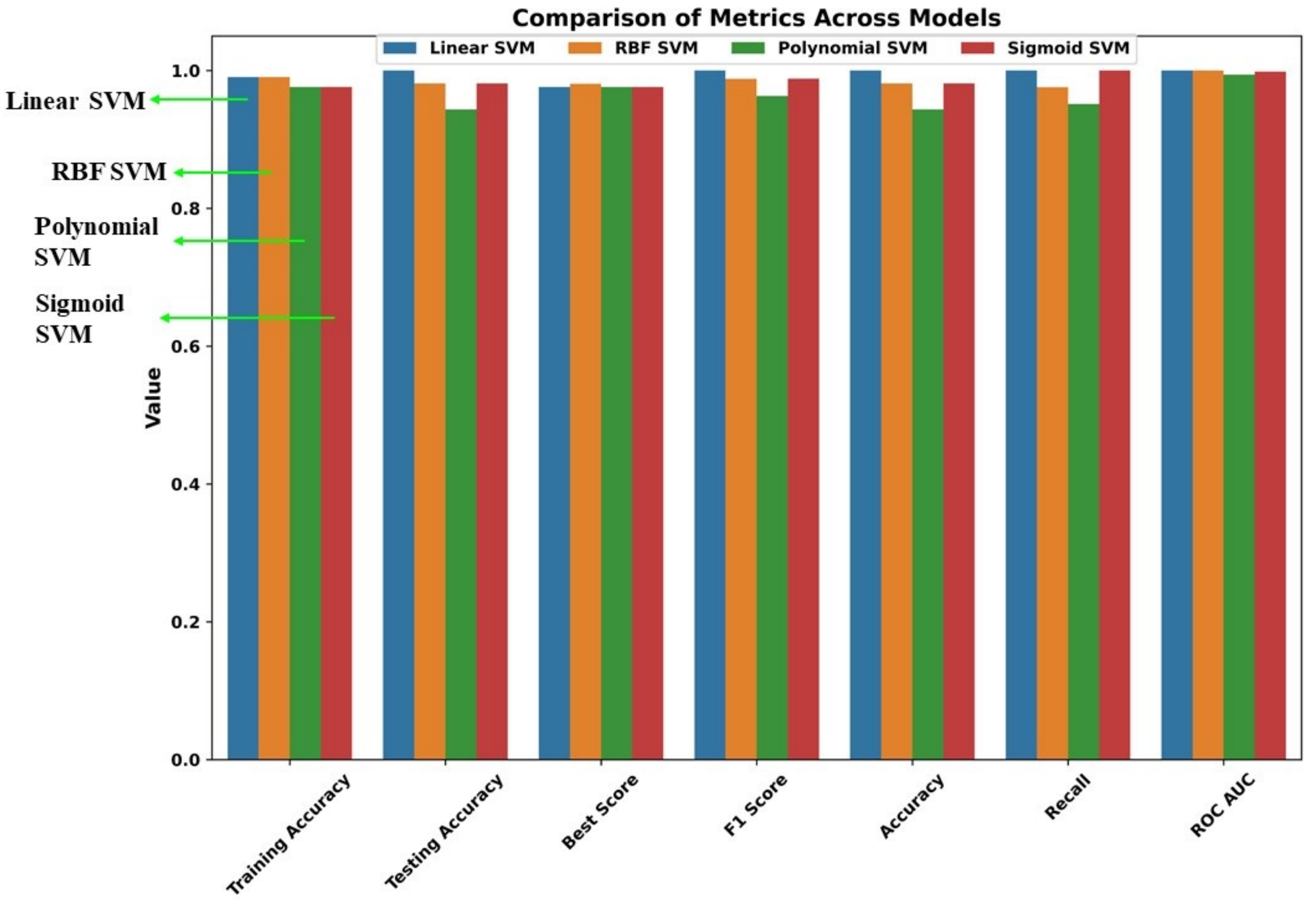

(a) Metric comparison across SVM models

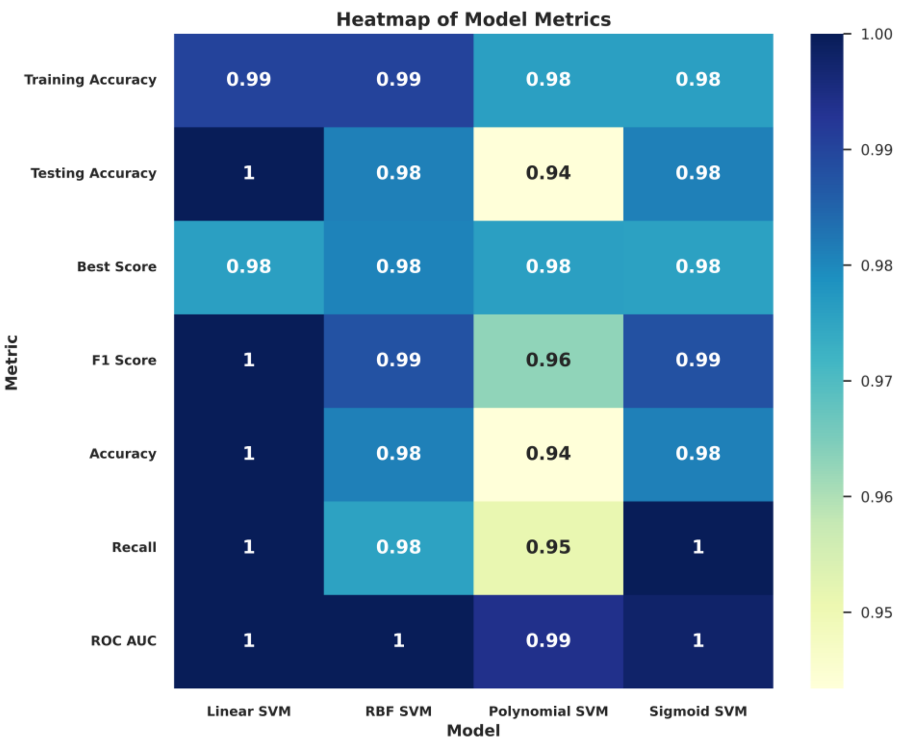

(b)Heatmap: SVM Models

Fig. 6. SVM Model Performance with CV (Scaled & Regularized)

The effectiveness of several Support Vector Machine (SVM) models is shown in the visualizations in Table IV. The first representation utilizes a bar chart to compare the training accuracy, testing accuracy, best score, F1 score, accuracy, recall, and ROC AUC of linear, RBF, polynomial, and sigmoid SVMs in Fig.6(a). The second plot is a heatmap illustrating the metrics for each model, highlighting their comparative strengths in Fig.6(b).

TABLE V
COMPARISON OF THE SVM MODEL'S ACCURACY PERFORMANCE FOR DIFFERENT CONDITIONS

Model	Data Scaling	Regularization	Cross Validation	Linear SVM	RBF SVM	Polynomial SVM	Sigmoid SVM
Raw	No	No	No	0.7736	0.7736	0.7736	0.7736
Scaled	Yes	No	No	1.0000	0.9623	0.9811	0.7736
Scaled & Regularized	Yes	Yes	No	1.0000	0.9811	0.9811	1.0000
CV, Scaled & Regularized	Yes	Yes	Yes	1.0000	0.9811	0.9434	0.9811

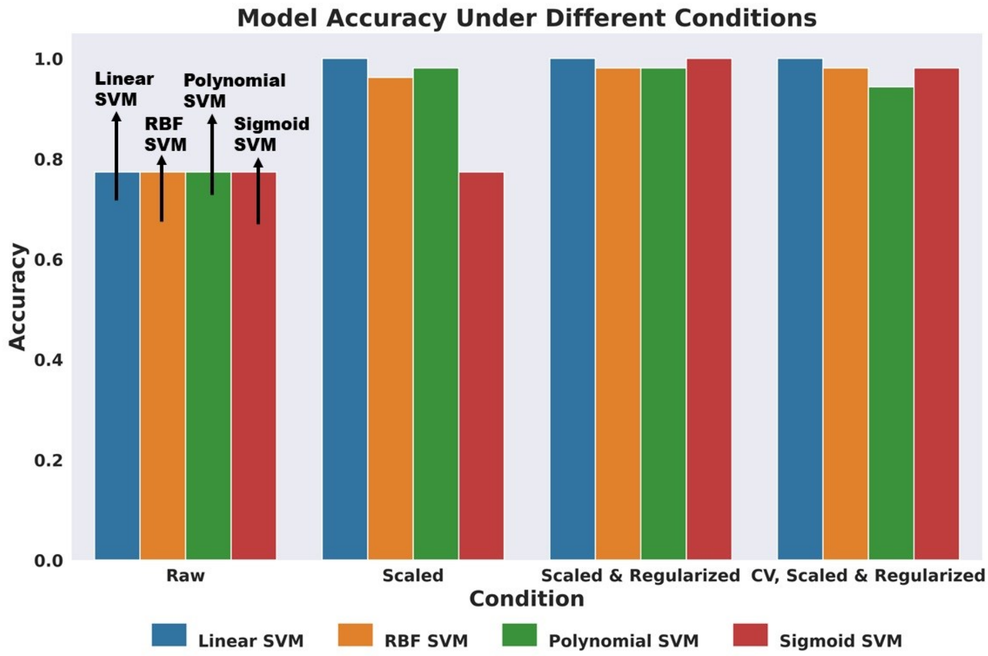

Fig. 7. SVM model's accuracy performance for different conditions

Accuracy results for several SVM kernels for various conditions are shown in Table V. By using scaling and regularization techniques, both linear and RBF SVMs achieve optimal accuracy are displayed in Fig. 7. Polynomial SVM has high accuracy but experiences a small decrease in performance during cross-validation. Scaling and regularization enable sigmoid support vector machines to closely resemble linear and RBF SVMs.

This study evaluated the precision of OCTID features using various SVM kernels under different preprocessing conditions are shown in Table VI. The linear SVM consistently achieved perfect accuracy (1.0) with scaled, regularized features and cross-validation (CV). The RBF SVM reached near-perfect accuracy (0.9762) with scaling and regularization, improving to 1.0 with CV. The sigmoid SVM peaked at 1.0 after scaling and regularization but decreased to 0.9762 with CV. Despite some inconsistency, the polynomial SVM maintained high accuracy across most scenarios.

This study analyzed the recall of OCTID features using various SVM kernels across several preprocessing settings. Both the linear and sigmoid SVMs always got a recall rate of 1.0, which means they worked perfectly in all situations, including raw, scaled, scaled with regularization, and used with cross-validation (CV) are shown in Table VII. When the features were in their original form and scaled using regularization, the RBF SVM showed a recall rate of 100%. The recall rate was reduced to 0.9756 after cross-validation and feature scaling. Except for cross-validation, the polynomial SVM achieved a flawless recall. Applying cross-validation further reduced the recall to 0.9512.

TABLE VI
OCTID FEATURES PRECISION USING VARIOUS SVM KERNELS

Model / Conditions	Raw	Scaled	Scaled & Regularized	CV, Scaled & Regularized
Linear SVM	0.7736	1.0000	1.0000	1.0000
RBF SVM	0.7736	0.9756	0.9762	1.0000
Polynomial SVM	0.7736	1.0000	0.9762	0.9750
Sigmoid SVM	0.7736	0.7736	1.0000	0.9762

TABLE VII
OCTID FEATURES RECALL USING VARIOUS SVM KERNELS

Model / Conditions	Raw	Scaled	Scaled & Regularized	CV, Scaled & Regularized
Linear SVM	1.0000	1.0000	1.0000	1.0000
RBF SVM	1.0000	0.9756	1.0000	0.9756
Polynomial SVM	1.0000	0.9756	1.0000	0.9512
Sigmoid SVM	1.0000	1.0000	1.0000	1.0000

TABLE VIII
OCTID FEATURES F1 SCORE USING VARIOUS SVM KERNELS

Model / Conditions	Raw	Scaled	Scaled & Regularized	CV, Scaled & Regularized
Linear SVM	0.8723	1.0000	1.0000	1.0000
RBF SVM	0.8723	0.9756	0.9880	0.9877
Polynomial SVM	0.8723	0.9877	0.9880	0.9630
Sigmoid SVM	0.8723	0.8723	1.0000	0.9880

TABLE IX
OCTID FEATURES ROC-AUC USING VARIOUS SVM KERNELS

Model / Conditions	Raw	Scaled	Scaled & Regularized	CV, Scaled & Regularized
Linear SVM	1.0000	0.9959	1.0000	1.0000
RBF SVM	0.9959	0.9959	1.0000	1.0000
Polynomial SVM	1.0000	0.9959	1.0000	0.9939
Sigmoid SVM	0.6382	0.9959	1.0000	0.9980

F1 scores of OCTID features utilizing multiple SVM kernels across various preprocessing conditions were investigated in this work and are displayed in Table VIII. The linear Support Vector Machine (SVM) attained flawless F1 scores (1.0) while using scaled and regularized features, together with cross-validation (CV). The RBF SVM and polynomial SVM demonstrated strong F1 scores, particularly after adjusting for size and regularization, and these scores only slightly decreased with the use of cross-validation. After using scaling and regularization techniques, the sigmoid Support Vector Machine (SVM) achieved a perfect F1 score but saw a minor reduction when performing cross-validation.

The ROC-AUC of OCTID features was determined using various SVM kernels and preprocessing conditions are displayed in Table IX. The linear, RBF, and polynomial SVMs achieved near-perfect or perfect ROC-AUC scores, particularly after scaling, regularization, and cross-validation (CV). The sigmoid SVM got much better after being scaled and regularized, going from a lower ROC-AUC (0.6382) to almost perfect scores after CV, with a small drop to 0.9980 after scaling.

Utilizing optical coherence tomography (OCT) images, diagnostic criteria for AMD include the following: True Positive (TP) when AMD is correctly identified, False Positive (FP) when normal images are mistakenly identified as AMD, True Negative (TN) when normal conditions are correctly identified, and False Negative (FN) when AMD cases are missed or misclassified as normal.

The linear SVM model achieved 100% accuracy, as it had no errors, with zero false negatives (FN) and zero false positives (FP). The RBF SVM model had a slight decrease in accuracy due to a single false positive. The polynomial SVM had a total of three errors, consisting of one false negative and two false positives, resulting in lower accuracy compared to the linear SVM. The sigmoid SVM had one error, specifically one false negative. This performance indicates better accuracy compared to the polynomial SVM but slightly lower than the linear SVM, as seen in Fig. 8.

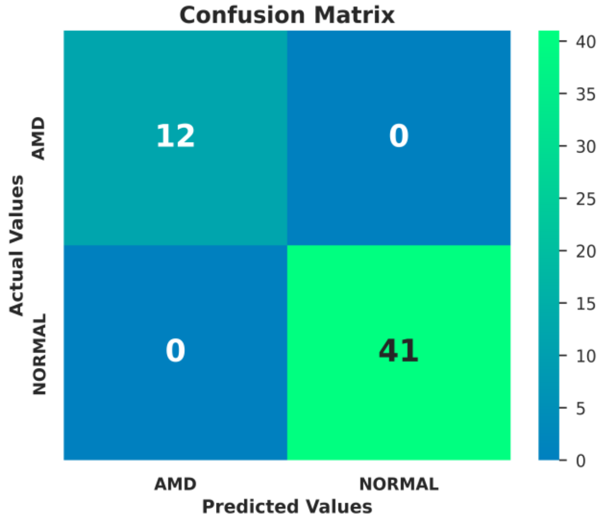

(a) Linear SVM

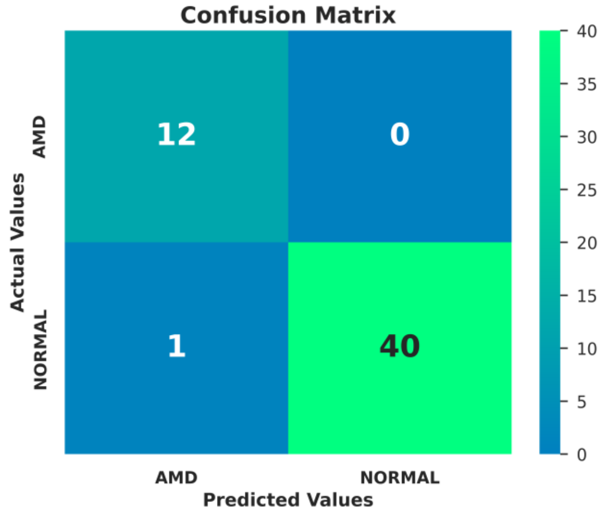

(b) RBF SVM

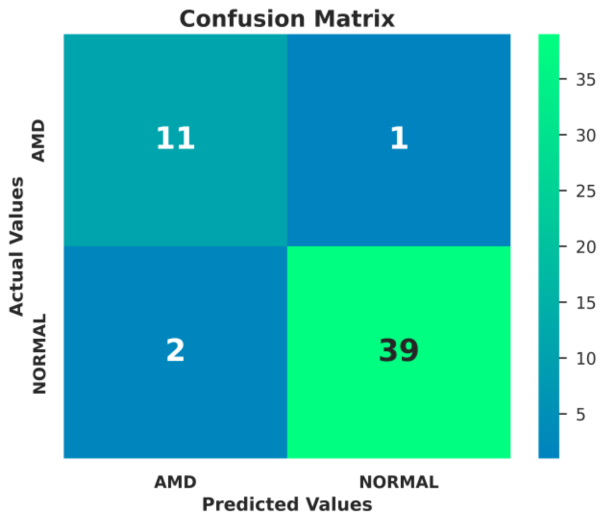

(c) Polynomial SVM

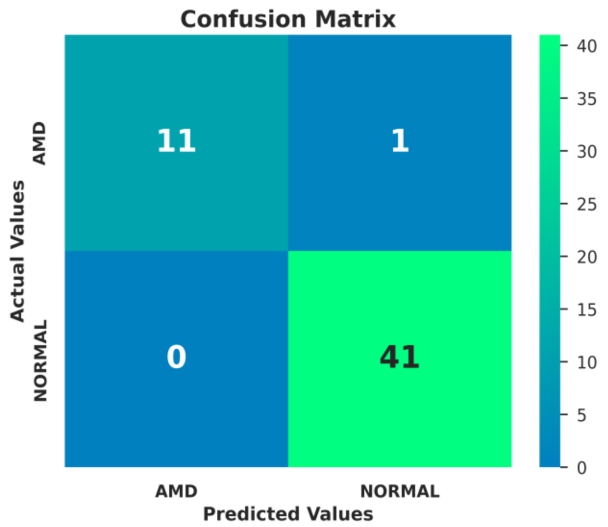

(d) Sigmoid SVM

Fig. 8. Confusion matrix of the SVM models

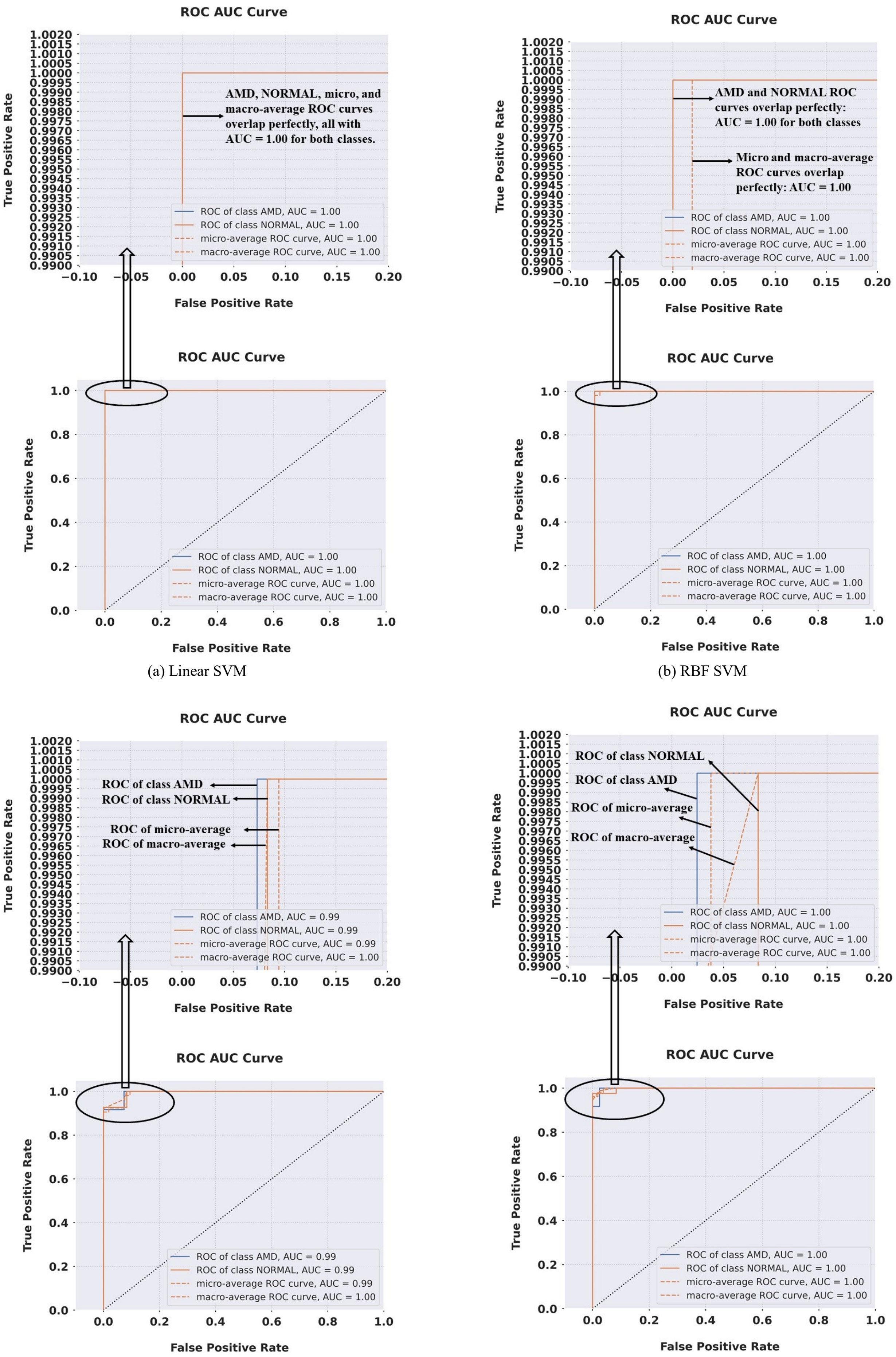

(a) Linear SVM (b) RBF SVM

(c) Polynomial SVM (d) Sigmoid SVM

Fig. 9. AUC ROC curve of the SVM model

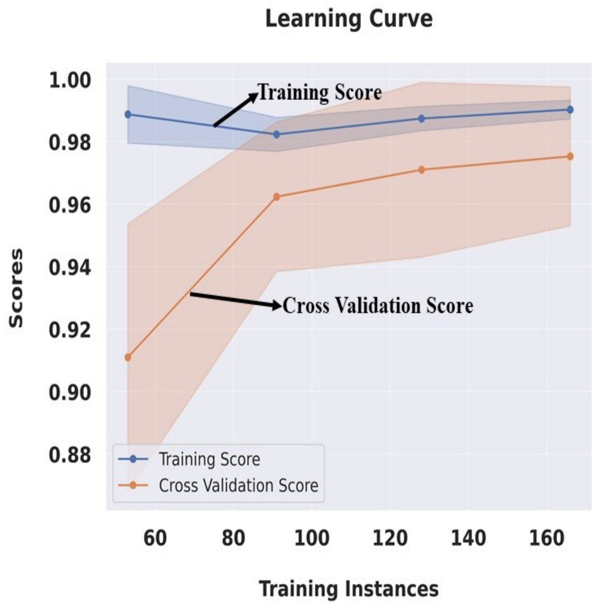

(a) Linear SVM

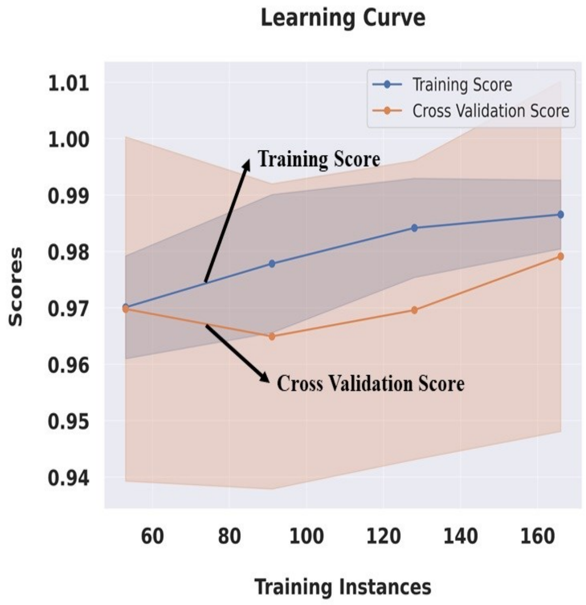

(b) RBF SVM

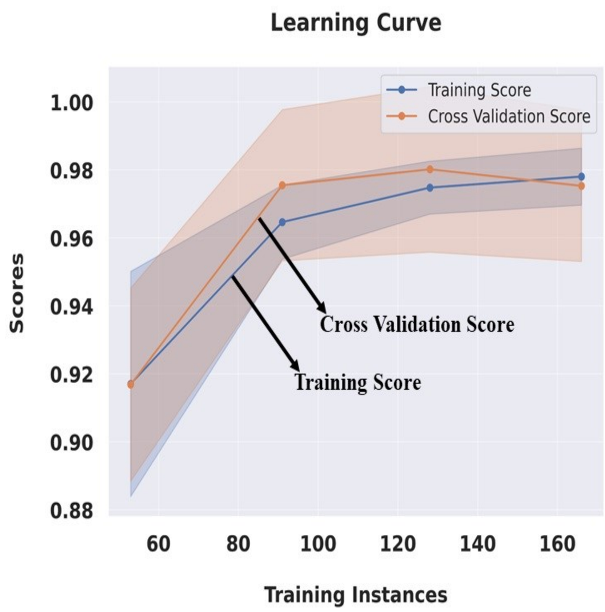

(c) Polynomial SVM

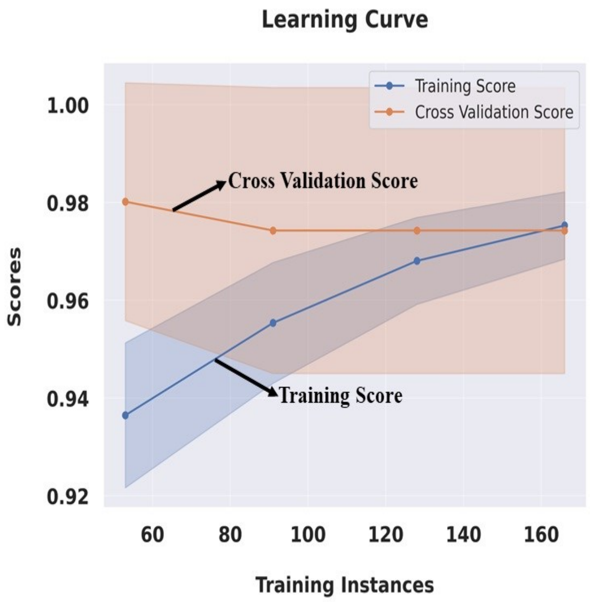

(d) Sigmoid SVM

Fig. 10. Learning curve of the SVM models

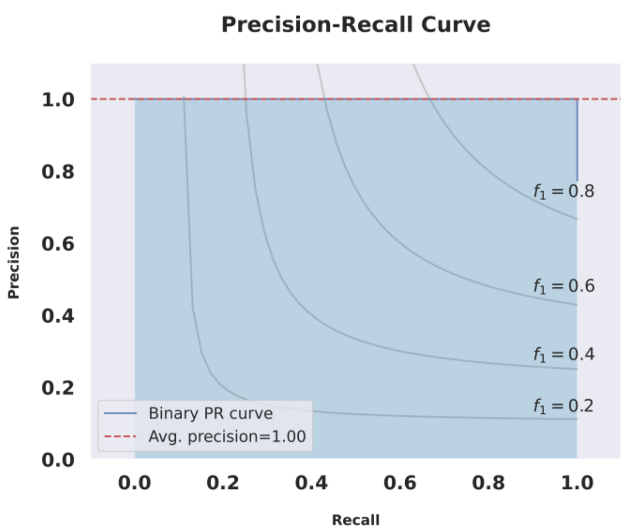

(a) Linear SVM

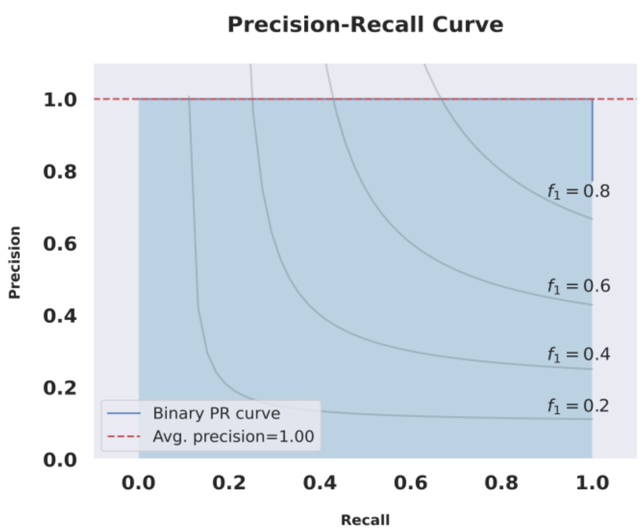

(b) RBF SVM

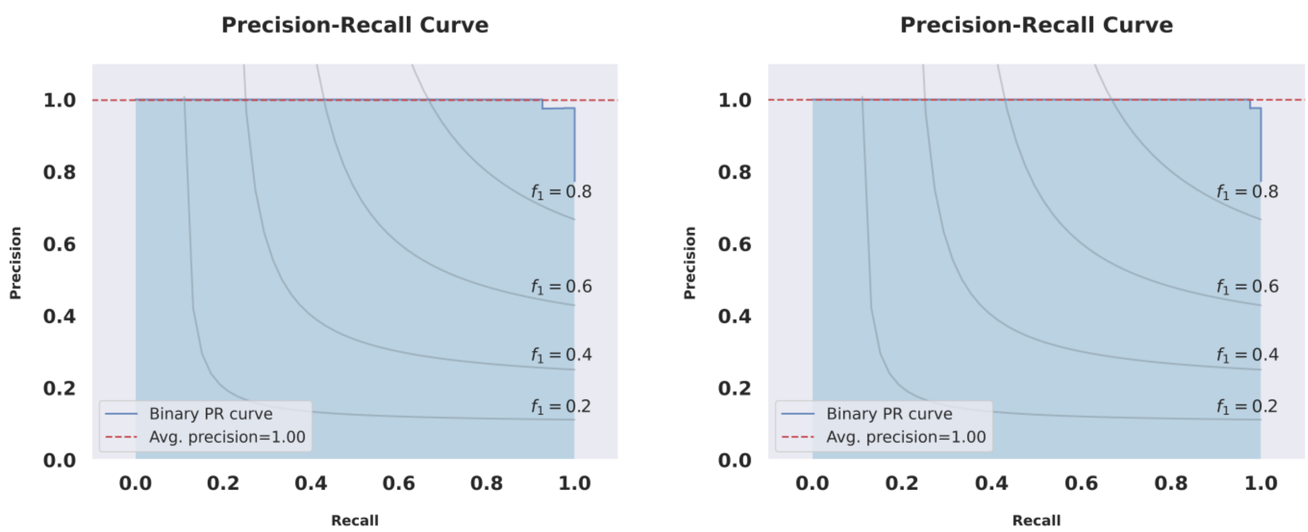

(c) Polynomial SVM

(d) Sigmoid SVM

Fig. 11. Precision recall curve of the SVM models

The linear SVM and RBF SVM models classified OCT images with a perfect AUC of 1.0, indicating the best performance for distinguishing between AMD and normal classes. The polynomial SVM also performed well, with a slightly lower AUC of 0.99. The sigmoid SVM showed strong performance as well, with an AUC of 1.0, though slightly lower than the RBF SVM, as illustrated in Fig. 9.

In OCTID binary classification, the SVM learning curve illustrates model performance as training data increases, highlighting potential overfitting or underfitting. The linear SVM (LSVM) shows excellent accuracy, with 99.04% on training and 100.00% on testing, indicating strong generalization. The Radial Basis Function SVM (RBF SVM) also performs well, with 99.04% train accuracy and 98.11% test accuracy. The polynomial SVM (PSVM) demonstrates decent performance, with 97.60% train accuracy and 94.34% test accuracy. The sigmoid SVM (SSVM), while achieving 97.60% train accuracy, slightly improves in testing with 98.11% accuracy, contrary to earlier expectations of poor performance. Overall, LSVM is the most accurate and robust, with PSVM performing well, while SSVM shows better generalization than initially anticipated, as shown in Fig. 10.

The linear SVM predicts consistently and accurately across all recall levels, achieving perfect precision (1.0) and recall (1.0). The sigmoid SVM also demonstrates strong performance with high precision (0.9762) and perfect recall (1.0). However, the polynomial SVM shows slightly lower precision (0.9750) and recall (0.9512), indicating a tradeoff between these metrics. The RBF SVM maintains perfect precision (1.0) but experiences a slight drop in recall (0.9756), as illustrated in Fig. 11.

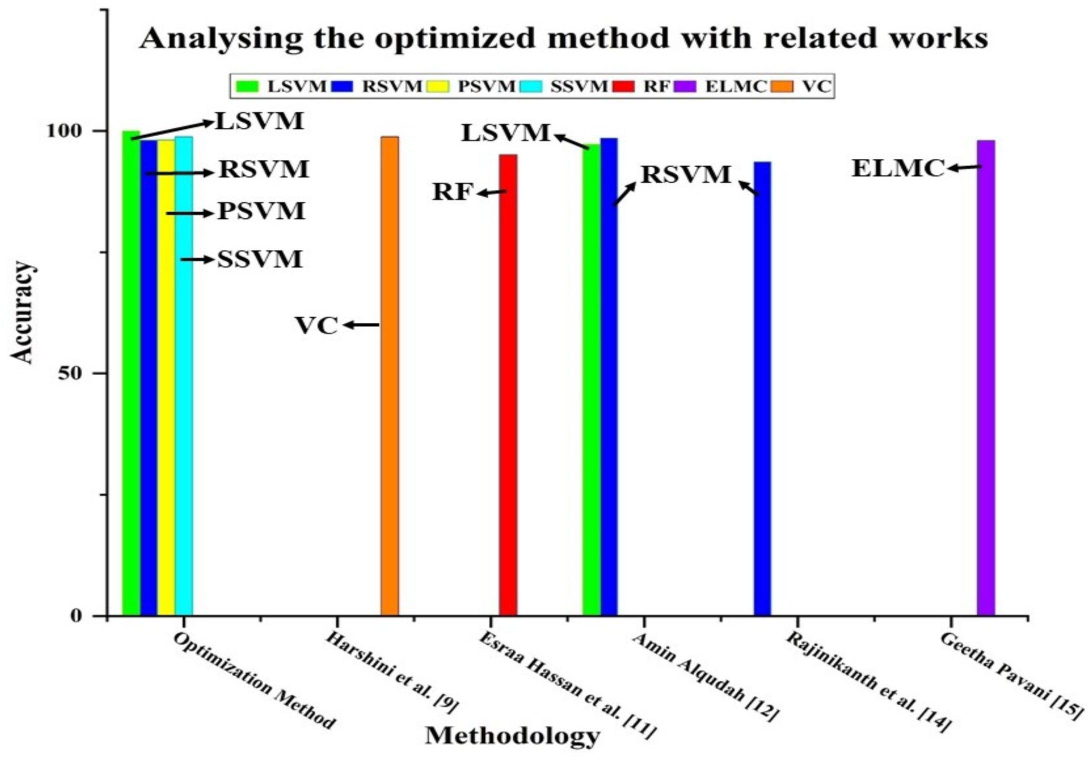

Fig. 12. Comparing the optimization method with the related works.

TABLE X
OCTID ACCURACY COMPARED WITH RELATED WORKS.

Literature	Classifier	Accuracy
Optimization Method	Linear: LSVM Nonlinear: RBFSVM Nonlinear: PSVM Nonlinear: SSVM	100% 98.11% 94.34% 98.11%
Harshini et al. [9]	Voting Classifier	98.79%
Esraa Hassan et al. [11]	Random Forest	95.10%
Amin Alqudah [12]	Linear SVM, RBF SVM	97.28%, 98.56%
Rajinikanth et al. [14]	RBF SVM	93.67%
Geetha Pavani [15]	ELM Classifier	98%

The linear SVM predicts consistently and accurately across all recall levels, achieving perfect precision (1.0) and recall (1.0). The sigmoid SVM also demonstrates strong performance with high precision (0.9762) and perfect recall (1.0). However, the polynomial SVM shows slightly lower precision (0.9750) and recall (0.9512), indicating a tradeoff between these metrics. The RBF SVM maintains perfect precision (1.0) but experiences a slight drop in recall (0.9756), as illustrated in Fig. 11.

The study compares SVM classifiers for diagnosing Age-related Macular Degeneration (AMD) using Optical Coherence Tomography images. The linear SVM achieved 100% accuracy across all preprocessing conditions, including scaling, regularization, and cross-validation. The RBF SVM performed well with a test accuracy of 98.11%, while the polynomial SVM achieved 94.34% accuracy. The Sigmoid SVM showed varying results, with improvements to 100% accuracy under scaling and regularization but dropping slightly to 98.11% with cross-validation. These findings highlight the crucial role of data preprocessing and model tuning in enhancing SVM performance for AMD classification. Table X compares the accuracy of OCTID to that of related models.

Comparatively, Harshini et al. used a voting classifier achieving 98.79% accuracy, while Esraa Hassan et al. reported 95.10% accuracy using a random forest classifier. Amin Alqudah's research found an accuracy of 97.28% for linear SVM and 98.56% for RBF SVM, proving SVM-based techniques work. Rajinikanth et al. used an RBF SVM and obtained 93.67% accuracy, slightly lower than other studies. Geetha Pavani's Extreme Learning Machine (ELM) classifier achieved 98% accuracy. Overall, the comparison in Fig. 12. shows that SVM models, especially RBF SVM, are highly effective for diagnosing AMD using OCT images. These findings support the use of SVM-based optimization methods in assisting ophthalmologists with AMD diagnosis.

V. Conclusion

VI. The current research intended to determine whether multiple Support Vector Machine (SVM) kernels performed in the normal and AMD retinal OCT classification of images. In the study on retinal OCT image classification, the Linear SVM (LSVM) achieved perfect accuracy (1.0) after data scaling and regularization, up from 0.7736, showcasing its effectiveness for linearly separable data. RBF and polynomial SVMs also performed well, with 0.9811 accuracy post-scaling and regularization, though they required careful parameter tuning. The sigmoid SVM improved from 0.7736 to 1.0 with regularization. These findings highlight the importance of data preparation and model adjustment, as optimal scaling, regularization, and cross-validation significantly enhance SVM performance across all kernels, especially in classifying complex medical images.

References

[1] H. Vyawahare and P. Shinde, "Age-related macular degeneration: Epidemiology, pathophysiology, diagnosis, and treatment," *Cureus*, vol.14, no. 9, 2022.

[2] D. S. Friedman, B. J. O'Colmain, B. Mu˜noz, S. C. Tomany, C. McCarty, P. T. de Jong, B. Nemesure, P. Mitchell, J. Kempen, and Eye Diseases Prevalence Research Group, "Prevalence of age-related macular degeneration in the United States," *Archives of ophthalmology*, vol. 122, no. 4, pp. 564-572, 2004.

[3] M. Gałuszka, D. Pojda-Wilczek, and I. Karska-Basta, "Age-RelatedMacular or Retinal Degeneration?," *Medicina,* vol. 59, no. 5, pp. 920,2023.

[4] M. Chaudhuri, Y. Hassan, P. P. S. B. Vemana, M. S. B. Pattanashetty, Z. U. Abdin, and H. F. Siddiqui, "Age-Related Macular Degeneration: An Exponentially Emerging Imminent Threat of Visual Impairment and Irreversible Blindness," *Cureus*, vol. 15, no. 5, 2023.

[5] X. Zhao, M. Luo, and Y. Chen, "Age-Related Macular Degeneration," in *Atlas of Swept Source OCT and OCT Angiography*, Y. Chen and X. Peng, Eds. Singapore: Springer, 2023, pp. 97-113.

[6] A. M. Alqudah, "AOCT-NET: a convolutional network automated classification of multiclass retinal diseases using spectral-domain optical coherence tomography images," *Medical & Biological Engineering & Computing*, vol. 58, pp. 41-53, 2020.

[7] S. Gowrisankaran, X. Song, G. Wollstein, J. S. Schuman, B. J. Antony, and H. Ishikawa, "OCT Image Classification of Glaucoma Using AutoML–A Code-Free Deep Learning Platform," *Investigative Ophthalmology & Visual Science*, vol. 64, no. 8, 2023.

[8] M. Adamopoulou, D. Makrynioti, G. Gklistis, and C. Koutsojannis, "Revolutionizing eye disease diagnosis with deep learning and machine learning," *World Journal of Advanced Research and Reviews*, vol. 18, no. 2, pp. 741–763, May 2023.

[9] G. Harshini, B. Dinesh Saradhy, K. Satya Sai Phani Kumar Varma, and V. Kumar Vadladi, "Machine Learning Approach for Various Eye Diseases using Modified Voting Classifier Model," in *2023 International Conference on Inventive Computation Technologies (ICICT)*, IEEE, pp.88-95, 2023.

[10] A. Shamsan, E. Mohammed Senan, and H. Salameh Ahmad Shatnawi, "Automatic Classification of Colour Fundus Images for Prediction Eye Disease Types Based on Hybrid Features," *Diagnostics*, vol. 13, no. 10, pp. 1706, 2023.

[11] E. Hassan, S. Elmougy, M. R. Ibraheem, M. Shamim Hossain, K. AlMutib, A. Ghoneim, S. A. AlQahtani, and F. M. Talaat, “Enhanced Deep Learning Model for Classification of Retinal Optical Coherence Tomography Images,” *Sensors*, vol. 23, no. 12, pp. 5393, 2023.
[12] A. Alqudah and A. M. Alqudah, “Artificial intelligence hybrid system for enhancing retinal diseases classification using automated deep features extracted from OCT images,” *International Journal of Intelligent Systems and Applications in Engineering*, vol. 9, no. 3, pp. 91-100,2021.
[13] X. Wei and R. Sui, “A review of machine learning algorithms for retinal cyst segmentation on optical coherence tomography,” Sensors, vol. 23, no. 6, 2023: 3144.
[14] V. Rajinikanth, R. Sivakumar, D. Jude Hemanth, Seifedine Kadry, Jnyana Ranjan Mohanty, S. Arunmozhi, N. Sri Madhava Raja, and Nguyen Gia Nhu, “Automated classification of retinal images into AMD/non-AMD Class—a study using multi-threshold and Gaussian filter enhanced images,” *Evolutionary Intelligence*, vol. 14, pp. 1163-1171, 2021.
[15] G. Pappu, B. Biswal, T.K. Gandhi, and M.V.S. Sai Ram, “Classification of neovascularization on retinal images using extreme learning machine,” *International Journal of Imaging Systems and Technology*, vol. 31, no. 3, pp. 1536-1550, 2021.
[16] H. Abdulrahman and M. Khatib, “Classification of retina diseases from OCT using genetic programming,” *International Journal of Computer Applications*, vol. 177, no. 45, pp. 41-46, 2020.
[17] K. Venkatraman and M. Sumathi, “Classification of retinal disorders based on fluid patterns in OCT images,” Indian Journal of Public Health Research and Development, vol. 10, no. 7, pp.1367–1370, 2019.
[18] P. K. Karn and W. H. Abdulla, “On machine learning in clinical interpretation of retinal diseases using oct images,” *Bioengineering*, vol.10, no. 4, 2023: 407.
[19] J. Cervantes, F. Garcia-Lamont, L. Rodr´ıguez-Mazahua, and A. Lopez, “A comprehensive survey on support vector machine classification: Applications, challenges, and trends,” *Neurocomputing*, vol. 408, pp. 189-215, 2020.
[20] P. Gholami, P. Roy, M. Kuppuswamy Parthasarathy, and V. Lakshminarayanan, “OCTID: Optical coherence tomography image database,” *Computers & Electrical Engineering*, vol. 81, 2020.
[21] F. Pedregosa, G. Varoquaux, A. Gramfort, V. Michel, B. Thirion, O. Grisel, M. Blondel, P. Prettenhofer, R. Weiss, V. Dubourg, J. Duchesnay, J. Vanderplas, “Scikit-learn: Machine learning in Python,” *Journal of Machine Learning Research*, vol. 12, 2011, pp. 2825-2830.